Key Engineering Materials
ISSN: 1662-9795, Vol. 1049, pp 29-35
doi:10.4028/p-Wg5agb

Submitted: 2025-12-19
Revised: 2026-03-01
Accepted: 2026-03-02
Online: 2026-04-15

Material Parameter Identification Using Bayesian Data Assimilation and Biaxial Tensile Test

Akinori Yamanaka[1,a*] and Shun Shimaoka[1,b]

[1]Department of Mechanical Systems Engineering, Tokyo University of Agriculture and Technology, 2-24-16, Naka-cho, Koganei, Tokyo, Japan

[a]a-yamana@cc.tuat.ac.jp, [b]s252517q@st.go.tuat.ac.jp, (*corresponding author)

Keywords: Bayesian data assimilation, Material modeling, Parameter identification

Abstract. This study proposes a Bayesian data assimilation approach to estimate material model parameters based on deformation fields measured via digital image correlation in a biaxial tensile test using a cruciform specimen. The anisotropy parameters and exponent of the Yld2000-2d yield function for a A5052P-H32 aluminum alloy are identified. The results indicate that the proposed method can estimate parameters with high accuracy—comparable to those identified via conventional multiaxial testing methods—while requiring only a single biaxial test. The proposed method offers an efficient framework for material modeling by minimizing a cost function via Bayesian optimization, enabling parameter identification from a single biaxial tensile test for sheet metal forming applications.

Introduction

To efficiently design sheet metal forming processes, one must improve the accuracy of numerical simulation models that reproduce the deformation behavior of metallic materials. Achieving this accuracy requires the precise identification of parameters for yield functions and hardening laws. In this study a material model that describes the elastoplastic deformation behavior of metals is used. The conventional approach to material modeling is based on mechanical testing under various stress states, including multiple uniaxial tensile tests and multiaxial stress tests such as biaxial tensile tests using cruciform specimens. In this approach, the parameters of the material model are identified by fitting the model to stress–strain responses or equiplastic work contours obtained from these experiments [1]. However, performing multiple mechanical tests under different loading conditions is time-consuming and experimentally demanding.

In this study, a method is proposed to estimate the parameters of a material model by applying a data assimilation approach based on Bayes' theorem—hereinafter referred to as Bayesian data assimilation (DA) [2]—to heterogeneous strain fields that arise on the surface of a cruciform specimen during a biaxial tensile test. The strain fields are measured using digital image correlation (DIC). It is demonstrated that this method enables the estimation of material model parameters using only the results of a single biaxial tensile test. Notably, the Bayesian DA method employed in this study, which is based on Bayes' theorem, is advantageous over conventional inverse methods such as the finite-element model updating [3] and virtual fields methods [4]. Specifically, DA allows the uncertainty inherent in experimental data to be rigorously incorporated into the Bayesian inference. Herein, the anisotropy parameters and exponent of the Yld2000-2d yield function [5] are estimated via biaxial tensile tests conducted using a simple cruciform specimen for a 5000-series aluminum alloy sheet with strain measurements obtained using DIC. Furthermore, it is demonstrated that employing the parameters estimated using the proposed DA method improves the predictive accuracy of the deformation behavior observed experimentally.

Experimental Methods

Biaxial Tensile Test. To obtain experimental data for estimating the parameters of the material model through DA, a biaxial tensile test using a cruciform specimen was conducted. A hydraulically controlled biaxial tensile testing machine, as shown in Fig. 1(a), was employed. The loads applied to

the specimens were measured using two load cells. To continuously capture the deformation of the specimen surface, a charge-coupled device (CCD) camera (DFK23U274, Image Source) was positioned above the specimen and sequential images were recorded at a sampling frequency of 5 Hz. The testing machine was operated using an in-house control code developed in LabView. The material used in this study was a commercially available A5052P-H32 aluminum alloy with a nominal thickness of 1.0 mm. The geometries of the specimens are shown in Fig. 1(b). The specimen was clamped over a 30 mm region. A random speckle pattern was applied to one side of the specimen using spray paint for strain measurements using DIC. As shown in Fig. 1(b), two strain gauges were attached to opposite sides of the specimen to control the testing machine. In the biaxial tensile test, the true stress ratio in the x- and y-directions was set to $\sigma_{xx} : \sigma_{yy} = 1{:}1$.

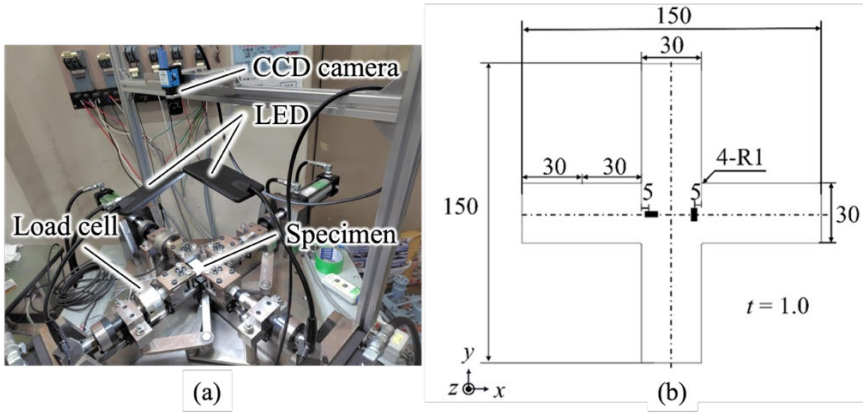

Fig. 1 (a) Biaxial testing machine and (b) dimensions of biaxial tensile specimen. Black rectangle in (b) shows strain gauge for controlling biaxial testing machine.

DIC. To measure the deformation field (i.e., the displacement and strain fields) using DIC, the resolution of the CCD camera was set to 1600 × 1200 pixels. To compute the deformation field from the captured images, image correlation software (GOM Correlate Professional 2021 Hotfix8 (GOM GmbH)) was used. The subset and step sizes were set to 19 and 15 pixels, respectively. Figure 2 shows the region of interest (ROI) specified for measuring the deformation field. A cruciform-shaped ROI was defined at the center of the specimen, excluding 1.5 mm from the edge of the specimen. At the measurement points indicated by red dots in Fig. 2, the displacements were recorded and used as the boundary conditions in the biaxial tensile test simulation.

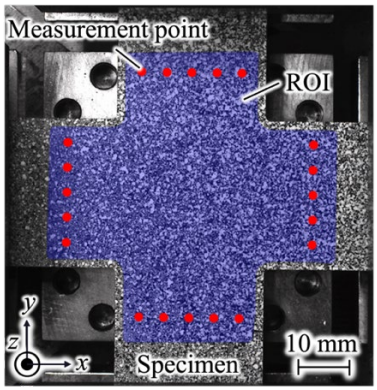

Fig. 2 Region of interest (ROI) to measure deformation field using digital image correlation.

Numerical Methods

Biaxial Tensile Test Simulation Using Yld2000-2d Yield Function. ABAQUS/Standard was used to perform a biaxial tensile test simulation corresponding to the experimental test. The geometry of the finite-element model was created by removing the gripping regions from the specimen shape, as

shown in Fig. 1 (b). The model was discretized into 8,418 elements with an approximate element size of 0.5, and reduced-integration shell elements were employed. The prescribed displacements were applied to each arm of the finite-element model. The Young's modulus and Poisson's ratio of the specimens were set to 63.347 GPa and 0.33, respectively. The Swift hardening law, expressed as $\sigma = c(a + \varepsilon^p)^n$, was employed to describe the strain-hardening behavior, where σ is the equivalent stress and ε^p is the equivalent plastic strain. The parameters of this hardening law were identified from a uniaxial tensile test conducted using A5052P-H32 aluminum alloy, which resulted in $c = 336.90$ MPa, $a = 5.01 \times 10^{-3}$, and $n = 0.143$. To implement the Yld2000-2d yield function in ABAQUS, the Unified Material Model Driver for Plasticity user subroutine [6] was employed. The Yld2000-2d yield function contains eight anisotropy parameters; it sets α_i (i = 1–8) = 1.0 and M = 8.0 as the initial estimation. The total simulation time was 650 s, and the strain fields were output every 65 s. The strain distributions at these time instants were compared with the experimentally measured strain fields obtained via DIC in the data assimilation process.

Bayesian DA Based on DMC-TPE. In this study, DA to minimize the cost function using the Data assimilation method Minimizing the Cost function with Tree-structured Parzen Estimator (DMC-TPE) method [2] was employed. In DMC-TPE, the evolution of the system state and its relationship with the experimental observations are formulated within a state-space model. The state vector $\boldsymbol{x}_t$ and observation vector $\boldsymbol{y}_t$ at time t are defined as follows:

$$\boldsymbol{x}_t = \left({\varepsilon_{xx}}^{1(t)}, \dots, {\varepsilon_{xx}}^{l(t)}, {\varepsilon_{yy}}^{1(t)}, \dots, {\varepsilon_{yy}}^{l(t)}, {\varepsilon_{xy}}^{1(t)} \dots, {\varepsilon_{xy}}^{l(t)}, \alpha_1, \dots, \alpha_8, M\right)^{\mathrm{T}} \quad (1)$$

$$\boldsymbol{y}_t = \left({\varepsilon_{xx}}^{1,\mathrm{obs}(t)}, \dots, {\varepsilon_{xx}}^{l,\mathrm{obs}(t)}, {\varepsilon_{yy}}^{1,\mathrm{obs}(t)}, \dots, {\varepsilon_{yy}}^{l,\mathrm{obs}(t)}, {\varepsilon_{xy}}^{1,\mathrm{obs}(t)} \dots, {\varepsilon_{xy}}^{l,\mathrm{obs}(t)}\right)^{\mathrm{T}} \quad (2)$$

Here, ${\varepsilon_{ij}}^{k(t)}$ denotes the ij ($i, j = x$ or y) component of strain at node k (k = 1, 2, …l) in the finite-element model of the cruciform specimen at time t; l is the number of nodes in the ROI; and ${\varepsilon_{ij}}^{k,\mathrm{obs}(t)}$ represents the corresponding strain component observed experimentally at the spatial location associated with ${\varepsilon_{ij}}^{k(t)}$.

As illustrated in Fig. 3, the misfit between the experimental results and numerical simulations is evaluated using the cost function, which includes the time integration of the misfit over time from t = 0 to $t = t_{\mathrm{end}}$.

$$J(\boldsymbol{x}_0) = \frac{1}{2}\left(\boldsymbol{x}_0 - \boldsymbol{x}_0^b\right)^{\mathrm{T}} \boldsymbol{B}^{-1}\left(\boldsymbol{x}_0 - \boldsymbol{x}_0^b\right) + \frac{1}{2}\sum_{t=0}^{t_{\mathrm{end}}}\left(\boldsymbol{y}_t - H_t(\boldsymbol{x}_t)\right)^{\mathrm{T}} \boldsymbol{R}_t^{-1}\left(\boldsymbol{y}_t - H_t(\boldsymbol{x}_t)\right) \quad (3)$$

Here, the superscript T denotes the transposed matrix, H_t is the observation operator that extracts the components from $\boldsymbol{x}_t$ corresponding to $\boldsymbol{y}_t$, and $\boldsymbol{x}_0^b$ is the initial estimate for $\boldsymbol{x}_0$; $\boldsymbol{B}$ and $\boldsymbol{R}_t$ are the error covariance matrices associated with the uncertainties of $\boldsymbol{x}_0^b$ and $\boldsymbol{y}_t$, respectively, and are referred to as the background and observation error covariance matrices, respectively. The first term on the right-hand side of Eq. (3) represents the deviation from the initial estimate, weighted by the background error covariance matrix, and therefore reflects the uncertainty associated with the prior parameter estimates. The second term corresponds to the time-integrated misfit between the experimentally measured strain field (obtained via DIC) and the strain field computed from the finite-element simulation, weighted by the observation error covariance matrix. The $\boldsymbol{x}_0$ that minimizes the cost function $J(\boldsymbol{x}_0)$ is regarded as the optimal state vector, which is denoted by $\boldsymbol{x}_0^a$, and the parameters contained in $\boldsymbol{x}_0^a$ are regarded as the optimal estimates. In this study, the minimization of J was performed using Bayesian optimization based on the TPE, which sequentially explores the admissible parameter space. The optimization is performed without explicitly computing the gradient of the cost function, as gradient evaluation for the present finite-element-based formulation is computationally complex. Instead, a surrogate model of the cost function is constructed using Gaussian process regression. The surrogate model is used to iteratively propose new candidate values of x_0 that are

expected to reduce the cost function, and this procedure is repeated until convergence. Therefore, $\boldsymbol{x}_0^a$ is obtained by repeating the following steps: (i) execute the biaxial tensile test simulation using the current estimate for $\boldsymbol{x}_0$, (ii) compute $J(\boldsymbol{x}_0)$ based on the simulation results, and (iii) update the estimate for $\boldsymbol{x}_0$ to reduce $J(\boldsymbol{x}_0)$. In this study, $\boldsymbol{B}$ is defined as follows:

$$\boldsymbol{B} = \text{diag.}\left(0, \ldots, 0, (S_{\alpha_1})^2, (S_{\alpha_2})^2, \ldots, (S_{\alpha_8})^2, (S_M)^2\right) \tag{4}$$

The initial strain in the specimen is assumed to be zero, and its variance is set to zero. Therefore, the first through $3l$-th components of $\boldsymbol{B}$ are zero. $S_{\alpha_i}(i = 1, 2, \ldots, 8)$ and S_M denote the standard deviations representing the uncertainties in the initial estimates for the anisotropy parameters α_i and the exponent M of the Yld2000-2d yield function, respectively. Assuming that the standard deviations are 30 % of the corresponding initial estimated values, $S_{\alpha_i} = 0.30$ and $S_M = 2.40$ are used. $\boldsymbol{R}_t$ is defined as follows:

$$\boldsymbol{R}_t = \text{diag.}\left((S_{\varepsilon_{xx}})^2, \ldots, (S_{\varepsilon_{xx}})^2, (S_{\varepsilon_{yy}})^2, \ldots, (S_{\varepsilon_{yy}})^2, (S_{\varepsilon_{xy}})^2, \ldots, (S_{xy})^2\right) \tag{5}$$

Here, $S_{\varepsilon_{ij}}(i, j = x \text{ or } y)$ denotes the standard deviation of the strain components. In this study, the strain distribution on the specimen surface prior to the start of testing was measured using DIC, and the standard deviations computed from these measurements were considered observation errors. $S_{\varepsilon_{xx}} = 4.56 \times 10^{-4}$, $S_{\varepsilon_{yy}} = 4.25 \times 10^{-4}$, and $S_{\varepsilon_{xy}} = 2.97 \times 10^{-4}$ are used.

The initial state of the specimen and the initial estimates for the parameters are expressed as follows:

$$\boldsymbol{x}_0^b = (0, \ldots, 0, 1.0, 1.0, 1.0, 1.0, 1.0, 1.0, 1.0, 1,0, 8.0)^{\mathrm{T}} \tag{6}$$

Eq. (6) indicates that the initial strain in the specimen is zero and that the initial estimates for the parameters were set to α_i (i = 1–8) = 1.0 and M = 8.0, assuming isotropic plastic deformation. During the minimization calculation of the cost function using Bayesian optimization, one must prescribe admissible ranges for the parameters to be estimated. In this study, these ranges were set to $0.7 \leq \alpha_i$ ($i = 1, 2, \ldots, 8$) ≤ 1.3 and $6.0 \leq M \leq 12.0$.

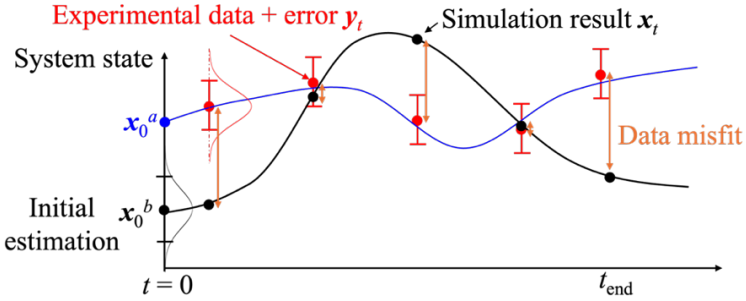

Fig. 3 Schematic illustration of Bayesian data assimilation (DA) based on DMC-BO.

Results and Discussion

Full-field Strain Measurement. Fig. 4(a) shows the distribution of the logarithmic strain measured using DIC. The arms of the specimens exhibited a uniaxial tensile state, whereas the central region showed a non-uniform strain distribution. The shear-strain components were concentrated near the corners of the specimens. Fig. 4(b) presents a scatter plot of the strain components in the principal strain space to evaluate the deformation field developed on the surface of the cruciform specimen. As shown in Fig. 4(b), many points corresponded to a uniaxial tensile state. By contrast, the strain values

associated with the equibiaxial tension were relatively low, and only negligible levels of simple pure shear strain were observed.

Parameter Identification and Verification. Among the 100 iterative calculations, the anisotropy parameter α_i and the exponent M of the Yld2000-2d yield function that resulted in the minimum value of the cost function were regarded as the optimal estimates. This computation was repeated five times as independent trials. This computation was repeated five times as independent trials using different random seeds for generating the prior samples in the Bayesian optimization procedure. Because Bayesian optimization relies on prior sampling, the results may depend on the initial random realization; therefore, multiple trials were conducted to assess the robustness of the parameter identification. Table 1 presents the optimal estimates obtained from the five trials. These optimal estimates were compared with previously identified reference values based on conventional mechanical testing [7]. The reference parameters reported in [7] were identified based on stress–strain data obtained from uniaxial tensile tests and hydraulic bulge tests. Although some of the optimal estimates exceeded 1.0, the corresponding reference values did not. By contrast, the estimated exponent had a value similar to the reference value.

Fig. 5 shows the yield surfaces computed using the Yld2000-2d yield function with both the optimal estimate and reference value. For the parameters obtained via DA, the yield surfaces were computed for each of the five independent trials, and the standard deviation of these surfaces is presented. The yield surface constructed using the reference value exhibited a more outwardly expanded shape and pronounced protrusion along the equibiaxial loading direction.

Fig. 6 presents the strain distributions obtained from the biaxial tensile test simulations using both the optimal estimate and reference value. Clearly, using the optimal estimate enables the quantitative reproduction of the deformation field observed in the experiment. This shows that the proposed DA approach can successfully estimate the parameters of the Yld2000-2d yield function with the same accuracy as those identified based on multiple material testing via only a single biaxial tensile test.

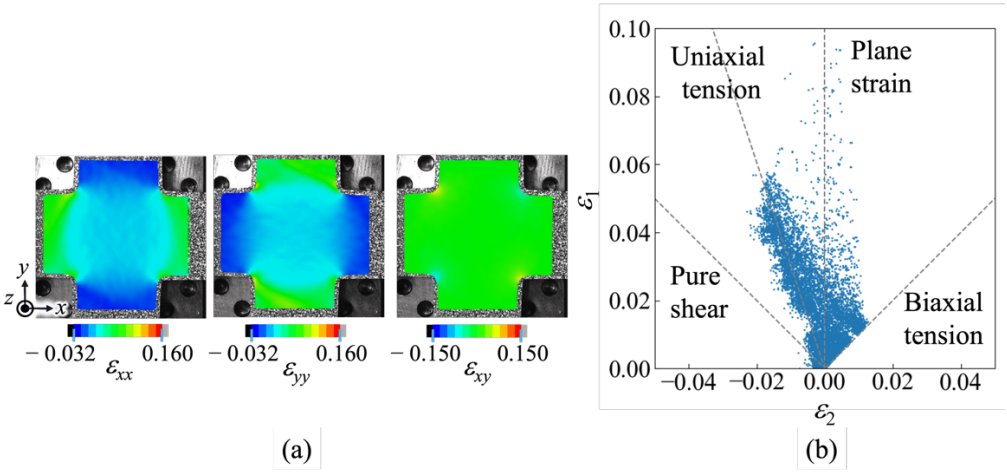

Fig. 4 (a) Distribution of logarithmic strains when true stress along x- and y-directions was $\sigma_{xx} = \sigma_{yy} =$ 242.2 MPa. Distribution of principal strain components is shown in (b).

Table 1 Optimally estimated anisotropic parameters and exponent of Yld2000-2d yield function obtained using proposed DA and reported in [7].

	α_1	α_2	α_3	α_4	α_5	α_6	α_7	α_8	M
Data assimilation	1.003	1.072	0.992	1.051	1.024	0.978	0.819	1.149	11.231
Reference	0.963	0.976	0.863	0.996	0.996	0.887	0.953	1.158	11.564

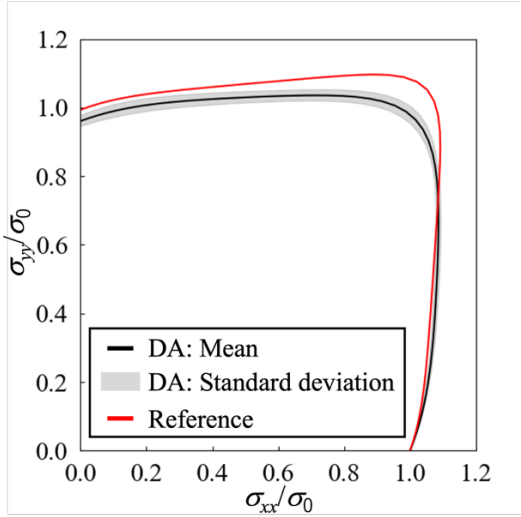

Fig. 5 Yield surface calculated using parameters estimated optimally using DA and reference values shown in Table 1.

Conclusion

In this study, a Bayesian DA method is proposed to estimate the parameters of a material model by assimilating the deformation field obtained via a biaxial tensile test using a cruciform specimen into a biaxial tensile test simulation. Using the proposed method, the anisotropy parameters and the exponent of the Yld2000-2d yield function were estimated for a A5052P-H32 aluminum alloy sheet. The results indicated that the parameters can be estimated with an accuracy comparable to that of the conventional approach, which requires multiple material tests, while requiring only a single biaxial tensile test. These findings contribute to the development of efficient material modeling and the design of sheet-metal forming processes.

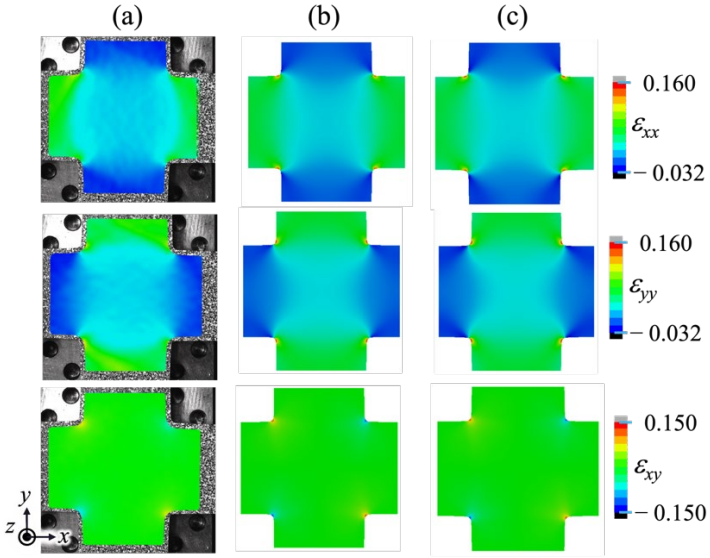

Fig. 6 Distribution of logarithmic strains when $\sigma_{xx} = \sigma_{yy} = 242.2$ MPa (a) measured using DIC and (b) calculated using reference values and (c) estimated values shown in Table 1.

References

[1] D. Yanaga, T. Kuwabara, N. Uema, M. Asano, Material modeling of 6000 series aluminum alloy sheets with different density cube textures and effect on the accuracy of finite element simulation, Int. J. Solid Struct. 49 (2012) 3488-3495.

[2] K. Sasaki, A. Yamanaka, Bayesian data assimilation for phase-field fracture simulation and full-field strain measurement using digital image correlation, Theor. Appl. Frac. Mech. 141 (2026) 105347.

[3] Y. Zhang, A. Van Bael, A. Andrade-Campos, S. Coppieters, Parameter identifiability analysis: Mitigating the non-uniqueness issue in the inverse identification of an anisotropic yield function. Int. J. Solids Struct. 243 (2022) 111543.

[4] A. Lattanzi, F. Barlat, F. Pierron, A. Marek, M. Rossi, Inverse identification strategies for the characterization of transformation-based anisotropic plasticity models with the nonlinear VFM. Int. J. Mech. Sci. 173 (2020) 105422.

[5] F. Barlat, J. C. Brem, J. W. Yoon, K. Chung, R. E. Dick, D. J. Lege, F. Pourboghrat, S. H. Choi, E. Chu, Plane stress yield function for aluminum alloy sheets-Part 1: Theory. Int. J. Plasticity. 19 (2003) 1297-1319.

[6] H. Takizawa, T. Kuwabara, K. Oide, J. Yoshida, Development of the subroutine library 'UMMDp' for anisotropic yield functions commonly applicable to commercial FEM codes. J. Phys. Conf. Ser. 734 (2016) 032028.

[7] Y. Saito, H. Takizawa, Modeling of yield surfaces for A5052 aluminum alloy sheets with different tempers by simplified identification method and its experimental validation. Mater. Trans. 64 (2023) 605-1613.